RSC Advances

PAPER

View Article Online
View Journal | View Issue

Cite this: *RSC Adv.*, 2022, **12**, 11282

Liposome-based nanocapsules for the controlled release of dietary curcumin: PDDA and silica nanoparticle-coated DMPC liposomes enhance the fluorescence efficiency and anticancer activity of curcumin†

Alaa K. Othman,[a] Riham El Kurdi,[a] Adnan Badran,[b] Joelle Mesmar,[c] Elias Baydoun[c] and Digambara Patra *[a]

Nanosystems with various compositions and biological properties are being extensively investigated for drug and gene delivery applications. Many nanotechnology methods use novel nanocarriers, such as liposomes, in therapeutically targeted drug delivery systems. However, liposome matrices suffer from several limitations, including drug leakage and instability. Therefore, the surface modification of liposomes by coating them or adding polymers has advanced their application in drug delivery. Hence, the prevention of drug release from the liposome bilayers was the main focus of this work. For this purpose, liposomes were synthesized according to a thin film hydration method by applying various surface modifications. Three different nanocapsules, N1, N2, and N3, were prepared using 1,2-dimyristoyl-*sn*-glycero-3-phosphocholine (DMPC), poly(diallyldimethylammonium)chloride (PDAA) polymer, and silica nanoparticles. PDDA and silica nanoparticles were coated on the surface of liposomes using a layer-by-layer assembly method, completely encapsulating curcumin into the core of the liposome. Fluorescence spectroscopy, TGA, DLS, XRD, SEM, and zeta potential methods were used to characterize the prepared nanocapsules. Interestingly, the fluorescence of curcumin showed a blue shift and the fluorescence efficiency was extraordinarily enhanced ~25-, ~54-, and ~62-fold in the N1, N2, and N3 nanocapsules, respectively. Similarly, encapsulation efficiency, drug loading, and the anticancer activity of dietary curcumin were investigated for the different types of DMPC nanocapsules. The drug efficiencies of the liposomes were established according to the release of curcumin from the liposomes. The results showed that the release of curcumin from the nanocapsules decreased as the number of layers at the surface of the liposomes increased. The release of curcumin follows the Higuchi model; thus, a slow rate of diffusion is observed when a number of layers is added. The better encapsulation and higher anti-cancer activity of curcumin were also observed when more layers were added, which is due to electrostatic interactions inhibiting curcumin from being released.

Received 5th January 2022
Accepted 9th March 2022

DOI: 10.1039/d2ra00071g

rsc.li/rsc-advances

1. Introduction

Nowadays, nanostructured materials, including liposome-mediated polymeric nanocapsules, are being widely studied and there have been calls for interdisciplinary research efforts. In general, nanocapsules are formed in small sizes, between 10 and 1000 nm.[1] They are made up of a shell within which specific substances or drugs can penetrate or be immersed.[2] Moreover, nanocapsules prepared using biodegradable polymers have been gaining interest due to their significant use in site-specific drug delivery systems.[3] Nanocapsules are considered the most effective substance carriers, as they can promote the stability of active substances and can be biocompatible with tissues and cells. These properties are the result of their subcellular size, which contributes to achieving more intracellular intake than other carriers systems.[4] In addition, nanocapsules have been shown to recover the solubility of lipophilic, poorly water-soluble compounds and to shelter unstable molecules from biological changes.

Common polymers, such as polyvinylpyrrolidone, polylactic/polyglycolic acids, poly-ε-caprolactone, and polyalkyl cyanoacrylates are widely used in modifying the surface of liposomal nanocapsules and as essential reagents in the preparation of

[a]*Department of Chemistry, American University of Beirut, Beirut, Lebanon. E-mail: dp03@aub.edu.lb; Fax: +9611365217; Tel: +9611350000 ext: 3985*
[b]*Department of Basic Sciences, University of Petra, P.O. Box 961343, Amman, Jordan*
[c]*Department of Biology, American University of Beirut, Beirut, Lebanon*

† Electronic supplementary information (ESI) available. See https://doi.org/10.1039/d2ra00071g

polymeric nanocapsules.[2] Poly(dimethyldiallylammonium chloride) (PDDA) is a cationic polyelectrolyte polymer, which can be used in the preparation of polymeric nanocapsules, but has not been well studied for this purpose.[5] It is very important in biomedical applications, especially in drug delivery since it is biocompatible and can circulate in the bloodstream for a certain time due to its high molecular weight. It is also easily administered and its method of synthesis is simple and cheap.[6]

Liposome-mediated polymeric nanocapsules are composed of a liquid core that acts as a reservoir for the drug[7] and a polymeric membrane.[8] They are synthesized using different synthesis routes, such as the layer-by-layer assembly method, polymerization techniques, or nanoprecipitation and emulsion diffusion methods.[9,10] Lipids have the ability to self-assemble in aqueous media, resulting in the formation of liposomes. These are small and spherical artificial vesicles that are composed of cholesterol and natural non-toxic phospholipids surrounding an aqueous core.[11,12] Moreover, phospholipids are surface-active and amphiphilic molecules. This amphiphilic property makes them applicable for use as emulsifiers and wetting agents. Phospholipid bilayers are the main constituents of liposomes and cell membranes.[12] Phospholipids can be either natural (such as soybean) or synthetic (such as 1,2-dipalmitoyl-*sn-glycero*-3-phosphocholine (DPPC) and 1,2-dimyristoyl-*sn-glycero*-3-phosphocholine (DMPC)). Research has also indicated that DPPC/DMPC liposomes could serve as effective delivery vehicles for inducing immune responses against glycosphingolipid antigens.[13] Furthermore, liposomes are intensively used as carriers for different molecules in the cosmetics, therapeutics, food, and pharmaceutical industries.[14] These nanocarrier systems are flexible, biocompatible, and have the ability to self-assemble and load large molecules. Besides, liposomes offer a wide range of physicochemical and biophysical characteristics that can be adjusted to suit their biological environment.[15,16] Liposomes have been proved to be effective in drug delivery release.[17] And different studies have been done on liposomes aiming to lessen drug toxicity and to target certain sites.[18] Hence, the use of liposomes helps in improving the stability, efficacy, and therapeutic index of a drug. In fact, drug delivery based on liposomal encapsulation exhibits lower toxicity of the entrapped drugs, adequate targeting and flexibility in binding to specific agents to attain their targets.[12]

Curcumin, a component of turmeric, is a phytopolylphenol pigment derived from the rhizome of *Curcuma longa*, which is a perennial herb that belongs to the ginger family (Zingiberaceae), and is widely used in food as a spice and coloring agent.[19] Curcumin consists of two aryl rings that are composed of *ortho*-methoxy phenolic OH functional groups. The presence of intermolecular hydrogen atom transfer allows equilibrium between the keto and the enol forms of curcumin.[20] Curcumin is barely soluble in water but is highly soluble in organic solvents such as ethanol, acetone and dimethylsulfoxide.[21] Extensive preclinical studies have specified the potent therapeutic effect of curcumin towards numerous diseases due to its various pharmacological and biological functions.[19] Among these, curcumin has been shown to exhibit antioxidant,[22] anti-inflammatory,[23] and anticancer[24] properties. Therefore, improving the bioavailability of dietary curcumin is of great importance. Recently, curcumin has been encapsulated in different matrices, such as DBPC liposomes,[25] DAPC liposomes,[26] and F108 polymer.[27] In this work, we have prepared different types of liposome-mediated PDDA nanocapsules using DMPC and tested the release of curcumin at different pH, assessed fluorescence spectral change, and investigated their anticancer activity, which have shown remarkably promising results.

2. Materials and methods

2.1 Materials

Curcumin, HS-40 colloidal silica, poly(diallyldimethyl ammonium chloride), 3-(4,5-dimethylthiazol-2-yl)-2,5-diphenyltetrazolium bromide (MTT), and ethanol were obtained from Sigma-Aldrich. DMPC was purchased from Avanti, chloroform was obtained from Sharlu, and buffer solutions (pH 4, 6, 7) from Fisher. All chemicals were used directly without further purification and were dissolved in double-distilled water except for curcumin and DMPC, which were initially dissolved in ethanol and chloroform.

2.2 Preparation of liposomal curcumin

The preparation of liposomal curcumin was done using the thin film hydration method. Initially, 1.84 g of curcumin were dissolved in 0.5 mL of ethanol and 0.5 mL of chloroform, which was then added to 10 mg of DMPC (dissolved in 2.5 mL of ethanol and 2.5 mL of chloroform). In a second step, the organic solvents were evaporated using a rotary evaporator at 60 °C, and monitored for thin film formation once evaporation was complete. Afterwards, the sample was kept in a vacuum oven for 1 hour at 40 °C to the complete evaporation of the organic solvents. Afterwards, 5 mL of buffer solution at different pH values (4, 6 and 7) was then added to the prepared sample. These 3 pH values were tested because drug release is affected by the pH and cancer cells are known to be acidic. In addition, the liposomes are pH sensitive; hence acidic pH affects their matrix more than basic pH because of the presence of a phosphate group (basic pK_a value). To ensure that the lipid film is hydrated and the final solution is completely homogeneous, the sample was vortexed and heated to 25 °C below the phase transition temperature of the liposome, and then kept in a sonicator for 20 minutes. Finally, a mini-extruder device from Avanti Polar Lipids (Merck, Germany) was applied using a 0.22 micron filter. The extrusion was applied 20 times at 25 °C in order to obtain small particle sizes of liposomal curcumin.

2.3 Preparation of nanocapsules

Three different nanocapsules were prepared as described below. In the first case, a polymer layer was added to the liposome surface (Scheme 1A). Nanocapsules N1 consisted of a liposomal curcumin layer with an additional polymer layer. For this, 3 mL of the final liposomal curcumin solution was mixed with 3 mL of PDDA (1 mg mL^{-1}). The solution was kept in a water bath at 34 °C for 30 min, followed by 30 min at room

temperature. After that, the sample was centrifuged at 15 000 rpm for 20 min at 20 °C, and 5 mL of buffer solution was added to the precipitate. In the case of nanocapsules N2, which consist of a liposomal curcumin–PDDA–silica–PDDA layer, silica nanoparticles were incorporated between two layers of polymer (Scheme 1B). For this, the N1 solution was centrifuged at 15 000 rpm for 20 min at 20 °C, and 5 mL of buffer solution was added to the pellet followed by sonication. In a second step, 30 mL of LUDOX silica nanoparticles were added and the sample was kept for 1 hour at room temperature, then centrifuged at 15 000 rpm for 20 min at 20 °C. After that, 3 mL of buffer solution and 3 mL of PDDA solution (1 mg mL^{-1}) were added to the sample, which precipitated, and were properly mixed using sonication. Finally, the sample was kept for 30 min at 34 °C, then for 30 min at room temperature, followed by centrifugation at 15 000 rpm for 20 min at 20 °C. The obtained N2 nanocapsules were dissolved in 5 mL of buffer solution for further study. Finally in the case of N3 nanocapsules, another layer of curcumin was added on the silica nanoparticles deposited in N2, to make a liposomal curcumin–PDDA–silica–curcumin–PDDA layer (see Scheme 1C). For this, curcumin (50 μM) was added after the addition of silica nanoparticles (as described above for the N2 capsules) and then centrifuged for 30 minutes at 15 000 rpm for 20 min at 20 °C. Afterwards, 3 mL of buffer solution and 3 mL of PDDA (1 mg mL^{-1}) were added and the solution was kept first for 30 min at 34 °C and then for 30 minutes at room temperature. Finally, the solution was centrifuged at 15 000 rpm for 20 min at 20 °C, and 5 mL of buffer was added to the precipitate. All these modifications were done using self-assembly procedures.

2.4 Characterization and spectroscopic analysis

To record the absorption spectra at room temperature a JASCO V-570 UV-Vis-NIR spectrophotometer was used. For fluorescence emission spectral measurement, a Jobin-Yvon-Horiba Fluorolog III fluorometer was used with resolution increments of 1 nm and 5 nm slit-width and the FluorEssence program was used for analysis. In this case a 100 W xenon lamp was used as the excitation source, and the detector was R-928 set at 950 V. For scanning electron microscopy (SEM) analysis, a Tescan Vega 3 LMU with an Oxford EDX detector (Inca XmaW20) was applied. For sample preparation, a few drops of the nanocapsule solution were deposited on an aluminum stub and coated with a carbon-conductive adhesive tape. A NanoPlus zeta potential/nano particle analyzer was used for zeta potential and dynamic light scattering measurements. A Bruker d8 discover X-ray diffractometer equipped with Cu-Kα radiation ($\lambda = 1.5405$ Å) was used for the X-ray diffraction (XRD) data collection where a Johansson-type monochromator was used. Netzsch TGA 209 in the temperature range of 30 to 800 °C with increments of 1 °C min^{-1} in an N_2 atmosphere was applied for thermogravimetric analysis (TGA).

2.5 Drug loading and encapsulation efficiency

Drug loading and encapsulation efficiency were calculated by measuring the absorbance of the released curcumin using a UV-visible spectrophotometer at $\lambda_{abs} = 425$ nm. In a first step, the absorbance measurement was done after each washing during the preparations for the different nanocapsules. In a second the step, the precipitate was dissolved in 1 mL of double-distilled water (DDW) and dried in a freeze dryer for 24 h. The mass of the dried precipitate was recorded using a microbalance.

The drug loading and encapsulation efficiency were established based on the equations below.[28]

$$\text{Drug loading}\% = \frac{\text{amount of curcumin in the capsule}}{\text{total mass of the capsule}} \times 100 \quad (1)$$

$$\text{Encapsulation efficiency}\% = \frac{\text{amount of curcumin in the capsule}}{\text{initial amount of curcumin}} \times 100 \quad (2)$$

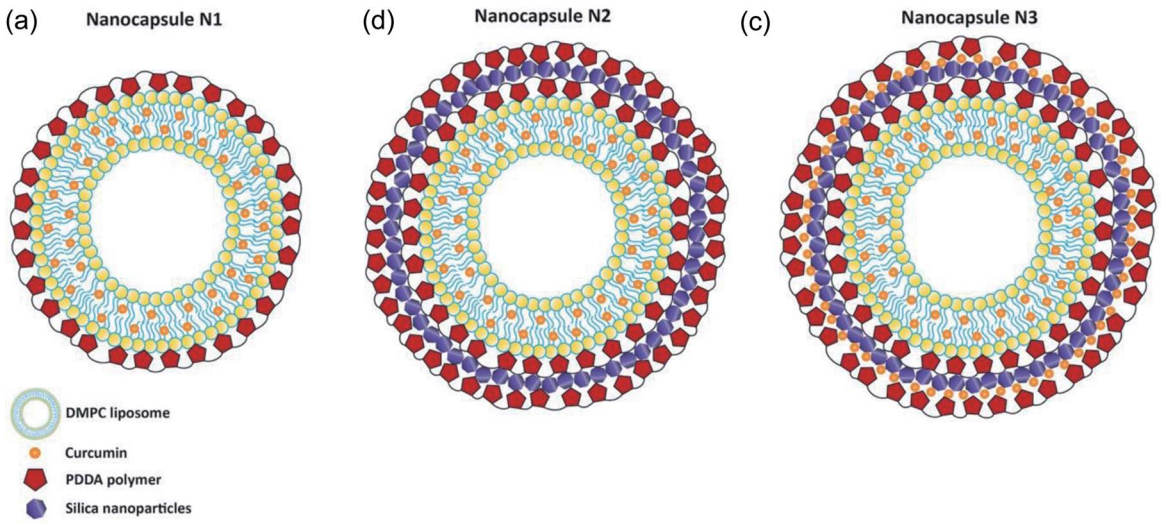

Scheme 1 An illustration of (a) nanocapsule N1, (b) nanocapsule N2 and, (c) nanocapsiles N3.

where the amount of curcumin in the nanocapsule is equal to the difference between the initial mass of curcumin used and the mass of unreacted curcumin present in the supernatant.

2.6 Release studies

After preparing the nanocapsules, the release of curcumin was studied at 37 °C according to human body temperature. For this, the nanocapsules were kept at 37 °C for 1 h and then centrifuged. The absorbance of the supernatant was measured. The precipitate was then resuspended in 5 mL of buffer solution, incubated for 1 h at 37 °C, and then centrifuged. This step was repeated several times for 2 days, and the absorbance of the supernatant was measured each time.

2.7 Cell cultures and viability assays

Human breast cancer cells MCF-7 (American Type Culture Collection; Manassas, VA) were maintained in complete Dulbecco's Modified Eagle's Medium (DMEM) high-glucose media, supplemented with 10% Fetal Bovine Serum (FBS) (both from Sigma-Aldrich, St. Louis, MO, USA), and 1% penicillin/streptomycin (Lonza, Switzerland), and kept at 37 °C in a humidified incubator (95% O_2 and 5% CO_2). MCF-7 cells (5×10^3) were seeded in 96-well plates and allowed to grow until they reached 30% confluency. The cells were then treated with the indicated concentrations of curcumin, silica, PDDA and the three different nanocapsules. The viability of the cells was measured with a 3-(4,5-dimethylthiazol-2-yl)-2,5-diphenyltetrazolium bromide (MTT; Sigma-Aldrich, St. Louis, MO, USA) reduction assay, 72 hours after treatment. Cell growth was determined as the proportional viability of the treated cells in comparison with the untreated control, the viability of which is assumed to be 100%.

3. Results and discussion

3.1 Spectroscopic analysis of the different nanocapsules

Resonance Rayleigh scattering (RRS), fluorescence emission, and UV-visible absorption spectra were recorded for N1, N2, N3 and free curcumin. For this, briefly, the precipitate of the nanocapsules was dissolved in 5 mL of PBS buffer solution of pH 7. In the case of free curcumin, 1.84 mg of curcumin was dissolved in 3 mL of ethanol and PBS mixture (1 : 10). In the first place, the RRS spectrum was measured by applying synchronous fluorescence spectroscopy (SFS) by keeping the

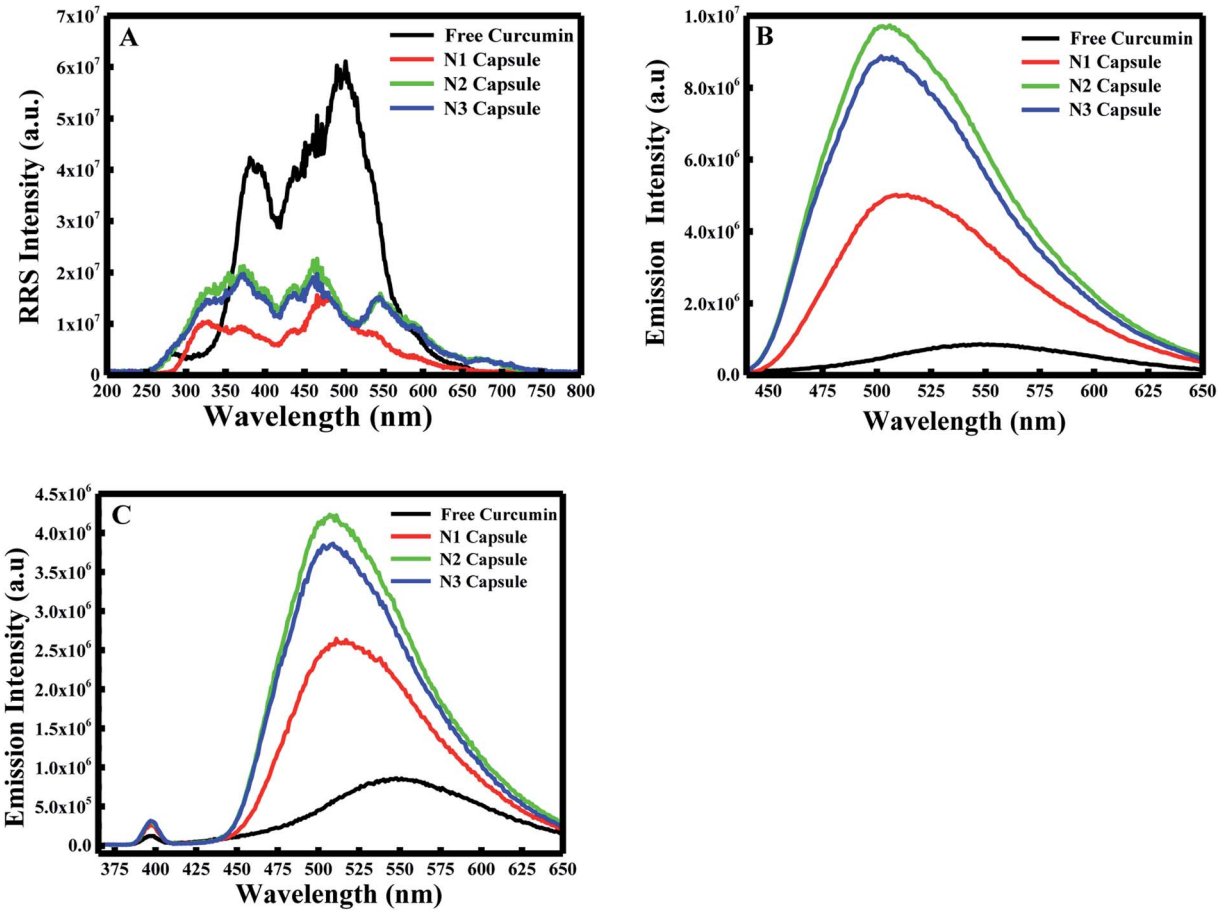

Fig. 1 (A) Resonance Rayleigh scattering spectra measured in synchronous fluorescence scan mode at $\Delta\lambda = 0$ nm, (B) fluorescence emission spectra excited at $\lambda = 425$ nm, and (C) fluorescence emission spectra excited at $\lambda = 350$ nm for free curcumin, N1, N2, and N3.

wavelength interval ($\Delta\lambda$) at 0 nm.[29] As shown in Fig. 1A, the RRS spectrum for free curcumin exhibited two significant peaks at ~380 nm and ~501 nm. But the 3 nanocapsules showed an additional two peaks at ~325 nm and ~548 nm. In comparison with the RRS peaks of curcumin, a blue shift was found from ~380 to ~370 nm and from ~501 nm to ~475 nm for the 3 NCs.

Furthermore, the fluorescence emission spectra were measured for the different components at excitation wavelengths equal to 425 nm (for the enol form of curcumin) and 350 nm (for the keto form of curcumin) in the emission ranges 440–650 and 370–650 nm, respectively. As shown in Fig. 1B and C, curcumin exhibited a major peak at λ = ~550 nm when excited at 425 nm and 350 nm. However, a blue shift was obtained from 550 nm to 510 nm for N1, N2 and N3 when excited at λ_{ex} = 425 nm. Similarly, a blue shift was also observed from 550 nm to ~525 nm for the three nanocapsules when excited at λ_{ex} = 350 nm. This blue shift is due to the change in polarity of the medium, which suggests curcumin is present in a more non-polar environment compared to free curcumin in an aqueous medium. A further polymer layer coating the surface of liposomal curcumin boosts the non-polar environment and allows curcumin to penetrate further into the hydrophobic pockets of the nanocapsules. Moreover, the fluorescence efficiency can be evaluated by estimating the relative fluorescence quantum yield (RFQY) for both emission spectra. This is established by taking the ratio of the fluorescence intensity to the absorbance at 425 nm of the fluorophore:[30]

The fluorescence spectra using RFQY at λ_{ex} = 425 nm and λ_{ex} = 350 nm are shown in Fig. 2A and B. The results showed that RFQY increases in intensity for the three nanocapsules, where the highest yield obtained was for N3 NCs. Hence, for N3 NCs, when excited at 425 nm and 350 nm the increase in RFQY was about 62 and 17 fold, respectively, compared to free curcumin, which also confirms that an increase in polymer layer coating allows curcumin to penetrate further into the hydrophobic pocket. Similarly, UV-visible absorption spectra were measured for these NCs, as shown in Fig. 3A, where the characteristic peak of curcumin alone was found to be sharp with a maximum at λ = 425 nm and a red shift was noticed from 425 to 428 nm for N1, N2 and N3 NCs. Although the absorption peak of the different nanocapsules tends to be broader, confirming the encapsulation of curcumin in the core of the liposomes. However, the relative absorbance for all three nanocapsules decreased compared to curcumin, with N1 showing the lowest absorbance, suggesting that a greater amount of curcumin was encapsulated in the N3 nanocapsules. The concentration of curcumin in the three nanocapsules was calculated according to the Beer–Lambert law (see ESI†). For N1 the curcumin concentration equals 15.01 μM, for N2 C = 16.94 μM and for N3 C = 17.43 μM.

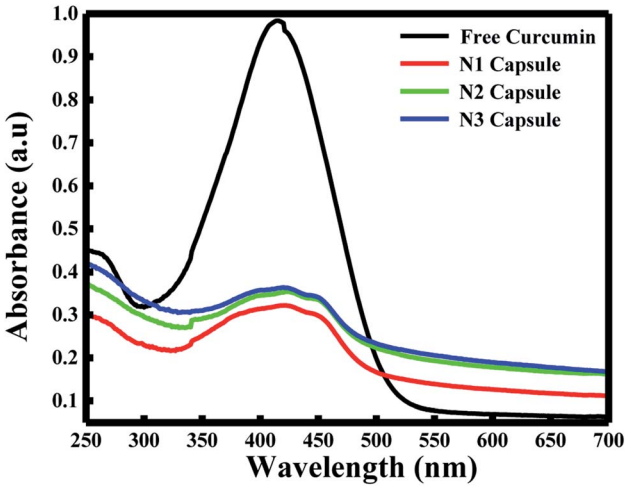

Fig. 3 UV-Vis spectra of free curcumin, N1, N2, and N3. All measurements were done for n = 3.

3.2 Drug loading and encapsulation efficiency

The concentration and the mass of un-encapsulated curcumin were calculated by using the curcumin calibration curve at pH 7. The percentage of drug loading and encapsulation efficiency of N1, N2 and R3 are depicted in Table 1. The calculations showed

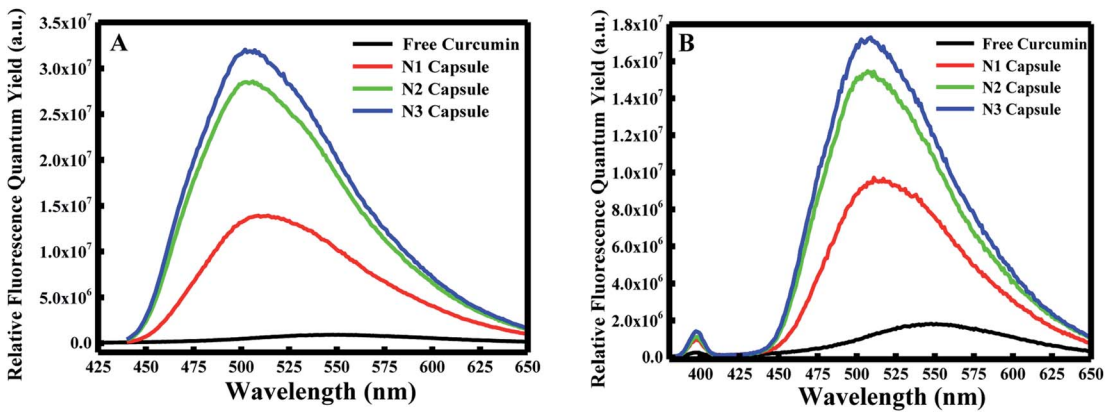

Fig. 2 (A) Relative fluorescence quantum yields excited at λ = 425 nm and (B) relative fluorescence quantum yields excited at λ = 350 nm for free curcumin, N1, N2, and N3.

Table 1 Relative drug loading and encapsulation efficiency percentages for N1, N2, and N3

Nanocapsule	Drug loading%	Encapsulation efficiency%
N1	43.8	92
N2	22.7	87
N3	22.5	86

nearly the same loading and encapsulation efficiency for N2 and N3 (87% and 86%, respectively). As for N1, 92% encapsulation efficiency was obtained. This highest value could be due to the fact that only one washing was made during the preparation of N1, while several washing steps were done while preparing N2 and N3, causing some loss of curcumin. The encapsulation efficiency results calculated in our experiment were similar to those obtained by Lee *et al.*, with a maximum encapsulation efficiency for curcumin of 93% (ref. 31) and higher than the values calculated by Young *et al.*, which were equal to 80%.[32]

3.3 Characterization techniques

The morphology of the prepared nanocapsules was established by scanning electron microscopy (SEM). N1, which was formed by self-assembly, showed random and non-uniform spherical shapes (Fig. 4A). However, after coating the surface of the nanocapsules with additional layers as in the case of N2 and N3, the PDDA and silica nanoparticles aggregated around them, giving them a uniform shape and smaller size compared to the N1 nanoparticles (Fig. 4B and C). Hence, the addition of extra layers tends to force the penetration of the curcumin molecule into the core of the liposomes (as confirmed earlier from the fluorescence spectra) and therefore induces the formation of smaller nanoparticles and their aggregation. Moreover, the particle size of the prepared nanocapsules was measured using dynamic light scattering (DLS). Each sample was diluted and sonicated before size analysis was carried out. The results are shown in Fig. S1A–C.† The nanocapsules sizes were 207 nm ± 12 nm, 297 nm ± 16 nm and 240 nm ± 15 nm for N1, N2 and N3, respectively. The differences observed in the three cases were around ±40 nm, which was due to the differences in aggregation and the different layers added. DLS results verify the aggregation present in the solution, since the SEM images give nanoparticles sizes of around 90 nm for N1 and 20–30 nm for N2 and N3.

To investigate the crystallinity of curcumin encapsulated in the three different DMPC nanocapsules, X-ray diffraction (XRD) was performed. The diffractograms of free DMPC lipid, free curcumin, N1, N2 and N3 are presented in Fig. S2A.† The XRD spectra of the free DMPC lipid illustrate the existence of three characteristic peaks at 6.4°, 15.7° and 21.3° and a number of minor peaks appeared in the 2θ range of 9–13.8°. The diffractogram of free curcumin shows significant peaks at 2θ equal to 8.06°, 9.20°, 12.46°, 14.95°, and 17.75° and some minor peaks with a 2θ range between 21.4° and 27.7°, which implies that curcumin is present in a crystalline form.[33] On the other hand, none of the nanocapsules showed XRD patterns with curcumin's characteristic peaks, expect for 21.4° observed in N2 and N3 nanocapsules. Moreover, the XRD patterns of N1, N2 and N3 were broad, suggesting that curcumin's significant XRD peaks became broader due to the addition of the different coating layers on the surface of the DMPC liposomal curcumin. This variety in the 2θ angle can be assigned to the changes in the crystallinity structure of curcumin, from a crystalline to an almost amorphous structure in the nanocapsules.[34,35] To study the thermal properties of pure curcumin and DMPC nanocapsules, thermogravimetric analysis (TGA) was performed, as depicted in Fig. S2B.† The results showed that no water loss occurred at 100 °C in N1, N2 or N3 nanocapsules. Pure curcumin showed thermal decomposition between 240 °C and 560 °C.[36] The obtained TGA patterns of the three different DMPC capsules demonstrated mass loss in the same temperature range. The main difference was in the % mass loss of the three nanocapsules. It was found that the % mass loss for N1, N2 and N3 nanocapsules were 64%, 54%, and 40%, respectively. This confirms the fact that curcumin was encapsulated more efficiently in N2 and N3 capsules, compared to N1.

3.4 Drug delivery release

Various approaches have been developed in order to increase curcumin delivery and protect it from degradation. Different kinds of therapeutic nanoparticles, such as liposomes, have been designed to improve curcumin's bioavailability and targeted delivery to specific cells.[35] Since curcumin is hydrophobic, it can be easily encapsulated within the liposome bilayer. The release of curcumin from the liposome bilayer depends on the surface of the nanocapsule and the pH of the medium. In this study, curcumin release was first investigated by studying the additive effect of the PDDA and silica layers (N1, N2 and N3). It was also determined by investigating the effect of pH for each of the nanocapsules.

3.4.1 Additive layer effects. In this study the UV-visible spectrophotometer technique was applied to monitor curcumin's release.[37,38] The release of curcumin from the nanocapsules was recorded by measuring the absorbance of curcumin at different time intervals. Curcumin's concentration was calculated based on the Beer–Lambert law. The release of curcumin for the N1, N2 and N3 nanocapsules at pH 7 is shown in Fig. 5. Hence, it is obvious that the release rate of curcumin is directly affected by the addition of the coating layers.[39] It was predicted that as the number of layers increases, curcumin release will decrease. And it is clear from the plot that faster release of the drug was assumed when the liposome surface was coated with the PDDA layer alone. The rate of curcumin release decreased when the silica nanoparticles were added and decreased further in the presence of curcumin and PDDA layers. Furthermore, in all three cases the drug release increased during the drug delivery mechanism, which was done over two consecutive days, reaching maximum release for N1 and minimum release for N3. Such layer-by-layer assembly enhances the stability of the nanocapsule due to the electrostatic interaction between the oppositely charged polymers and the surface of the nanocapsule.[40] Consequently, the stability of the nanocapsule increases when its surface is coated with more

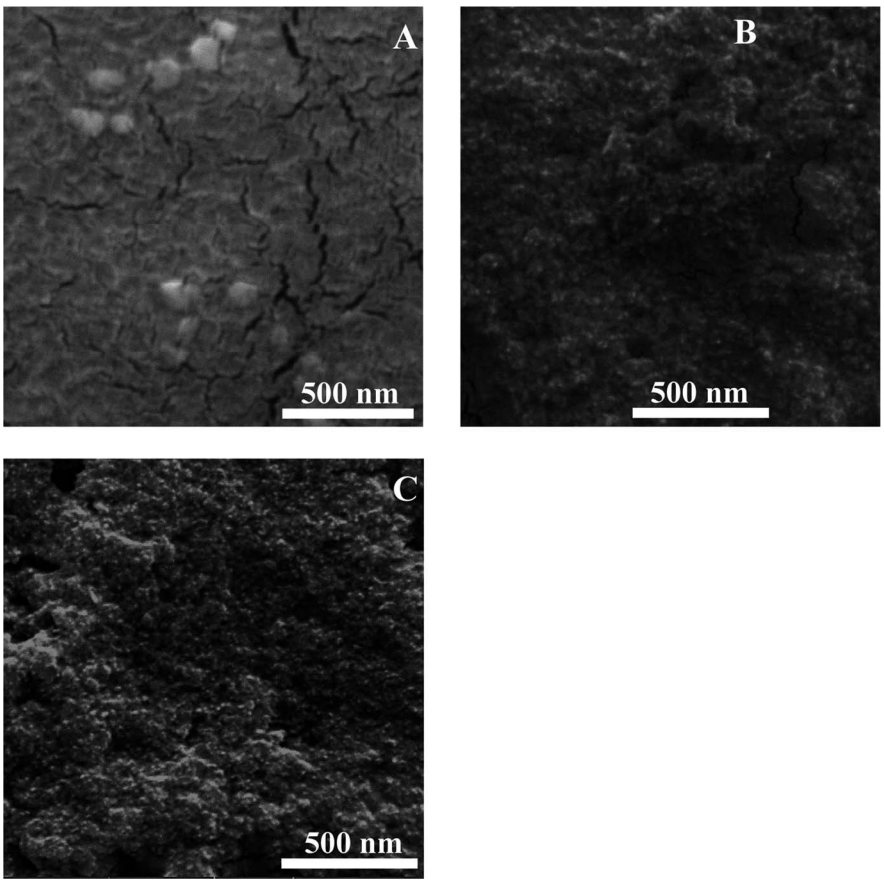

Fig. 4 SEM images of (A) N1, (B) N2, and (C) N3.

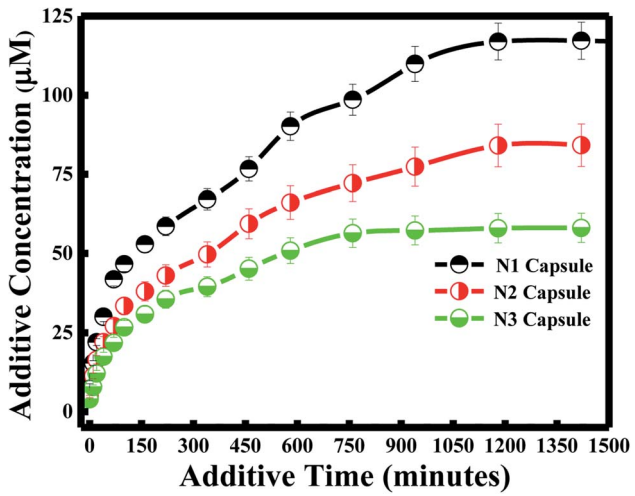

Fig. 5 Effects of additive layer on the release of curcumin from N1, N2, and N3 at pH 7. For all experiments, $n = 3$.

layers, as shown by our results. In the case of N2, when silica was incorporated between two polymeric layers, electrostatic interactions became stronger, due to the interaction of the negatively charged silica nanoparticles with the two layers of the PDDA polymer. Moving to N3, the addition of curcumin just after silica delayed the release of curcumin encapsulated within the liposome. Hence, the multiple layers boost the diffusion distance, thus hindering contact between the drug and the release media and consequently delaying curcumin release.[41]

3.4.2 Effects of pH. Different layers were added to the nanocapsules in order to obtain N1, N2 and N3. However, all the nanocapsules were at the end coated with a PDDA layer. Therefore, any modification in the pH will initially alter the final PDDA layer. Testing the surface charge is a dominant role which could have an extreme effect on the mode of release of the encapsulated agent.[42] The effects of three different pH values (4, 6 and 7) were tested accordingly by zeta-potential titration analysis in order to understand the mode of interaction between each layer in the different nanocapsules and to examine the release of curcumin (Fig. 6A–C). The drug release graphs show the concentration of curcumin over a period of 24 hours, which was determined based on the calibration curves of curcumin at pH 4, 6 and 7 using the Lambert–Beer law.

Zeta potential measurements of curcumin showed that the surface of curcumin is positively charged at pH = 4 (see Table 2), while it is negatively charged at pH 6 and 7. And the highest release of curcumin was observed with pH 4, while medium release was observed at pH 6, and the lowest release was at pH 7 for all three nanocapsules. Therefore, acidic conditions (pH = 4) promote high delivery of curcumin from

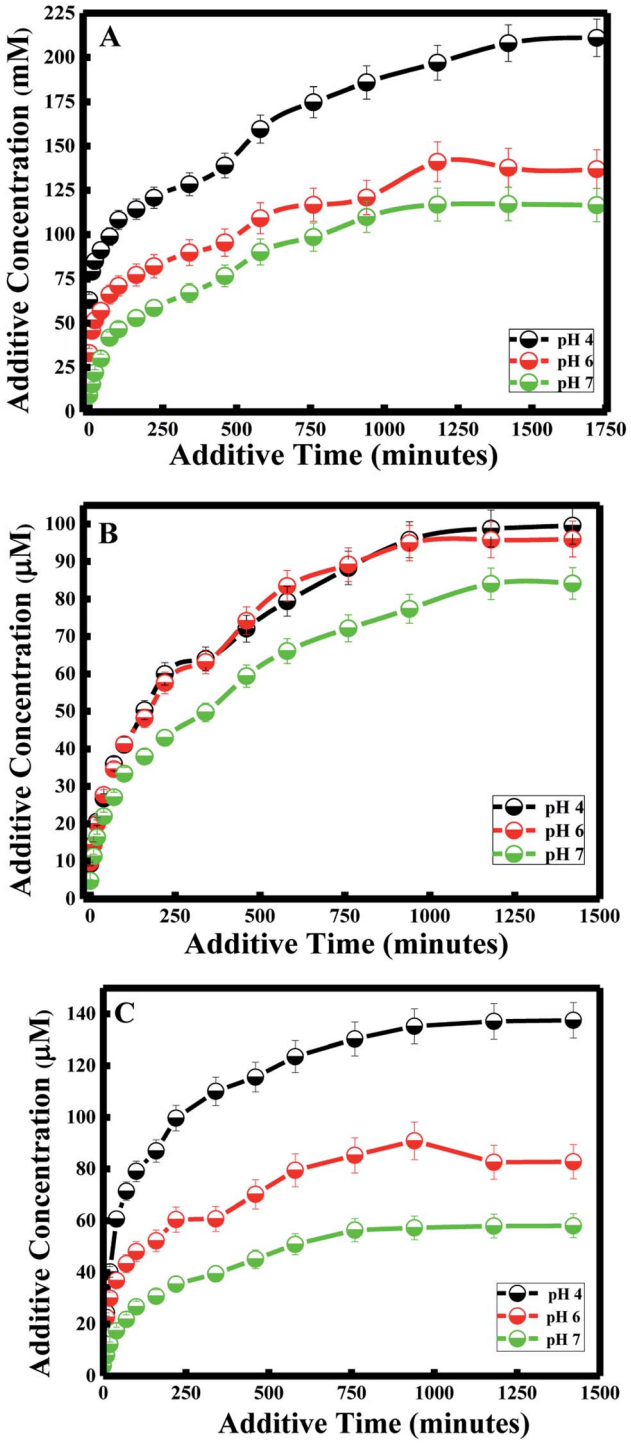

Fig. 6 Drug release from (A) N1, (B) N2, and (C) N3 at pH 4, 6, and 7. For all experiments, $n = 3$.

the nanocarrier system. This is due to the same positively charged surface of both curcumin and the PDDA surface of the nanocapsule at pH 4, which induces the inhibition of entrapment in the membrane. Studies have shown that tumor tissues contain acidic gradients different from normal tissues.[43] In addition, it was demonstrated that the cellular surface of malignant tissues is negatively charged.[44] Thus, from our studies, high cellular uptake of curcumin by tumor cells would be expected due to electrostatic interactions between curcumin and the cell surface. Additionally, recent results have emphasized that positively charged nanoparticles are preferentially absorbed by malignant tissues[45] and stored for a longer period of time, in comparison to nanoparticles with negative or neutral surfaces.[46]

Table 2 Zeta potential values for free curcumin, N1, N2, and N3

	Nanocapsule			
pH	N1	N2	N3	Curcumin
4	+23.9	+42.8	+44.7	+2.3
6	+25.4	+24.5	+22.7	−2.3
7	+21.8	+30.3	+31.9	−4.1

Under less acidic conditions (pH 6 and pH 7), curcumin demonstrated lower drug release. Zeta-potential measurements showed that the membrane surface of the nanocapsules was positively charged and that of curcumin was negatively charged at pH 6 and 7. Thus, the electrostatic interaction between the oppositely charged particles of the drug and nanocapsule enhanced the encapsulation efficiency of curcumin. Although curcumin remained entrapped in the nanocapsule during the drug delivery process, the release of curcumin at pH 7 was lower than the release at pH 6. This difference in drug release is due to the highest surface charge being obtained at pH 7 for the three nanocapsules (see Table 2).

In general, a large positive value zeta potential value reflects good and high physical stability of nanocapsules due to electrostatic repulsion of individual particles. Hence, when the zeta potential value is greater than +30 mV, it is generally considered to have sufficient repulsive force to attain better physical colloidal stability, enhancing the encapsulation of a drug and thereby lowering its release. On the other hand, a small zeta potential value can result in particle aggregation and flocculation due to the van der Waals attractive forces and thereby higher release of the drug.[47] Moreover, the drug release study at pH 4 and 6 did not have any effect on the nanocapsule itself, since lower release of curcumin was also obtained for N3 at pH 4 and 6, similar to the results obtained at pH 7 described in the previous section.

Furthermore, the kinetics for curcumin release were established based on the Higuchi model.[48] The equation proposed by Higuchi is as follows:

$$R = K_H \times t^{1/2}$$

where R is the amount of curcumin released, K_H is the Higuchi dissolution constant and t is the time in minutes. This equation demonstrates that the percentage release of curcumin is directly linked to a physical constant based on a simple diffusion act. As shown in Fig. S2 (see ESI†), it was found that there is a linear relationship between the quantity of curcumin released and the time considered. The Higuchi constant was calculated based on the slope value found for each linear fit (see Table S1, ESI†). Interestingly, the K_H value remains constant for the three

nanocapsules at different pH values. Thus, the K_H value for N1 was equal to 3.79864; this value decreased about ~2 fold with an increase in layers. The decrease in Higuchi dissolution constant indicates that a slow rate of diffusion occurred for curcumin in N3 NCs. Mainly this is due to the presence of several layers inhibiting the release of curcumin from the liposomes. The results obtained were in accordance with the data obtained by Pamunuwa *et al.* who studied the release of curcumin from different positive and negative lipids.[49]

3.5 Cytotoxicity study by MTT proliferation assays

In a recent study, the IC_{50} of curcumin was shown to be 25 ± 5.2 μM.[50] This concentration was sufficient to kill 50% of cancer cells in 48 hours. To establish the effect of the different nanocapsules on breast cancer, 25 μM of N1, N2, N3, curcumin, silica nanoparticles, PDAA and DMPC liposomes were used to treat MCF-7 breast cancer cells within 72 hours using the MTT proliferation assay. As shown in Fig. 7, N3 exhibited the highest percentage of cell growth inhibition, with 90% of cells killed within 72 hours. N1 and N2 showed 73 and 87% growth inhibition. The difference in the growth inhibition effect between the three nanocapsules is related to the percentage of curcumin encapsulated in the core of the liposomes. Moreover, curcumin alone killed only 57% of the cancer cells, suggesting that nanoencapsulation enhances the effect of curcumin as an anticancer reagent. The efficiency of our N3 nanocapsules was compared with other anticancer agents used to inhibit the proliferation of MCF-7 cancer cell (Table 3). It is also true that N3 exhibited the highest toxicity despite the release of N3 reaching a plateau at ~1200 min, which is not the fastest compared with N1 and N2. This could be due to the effect of polymer PDDA that enhances the anti-cancer activity of curcumin, as observed earlier by Bechnak *et al.*[27]

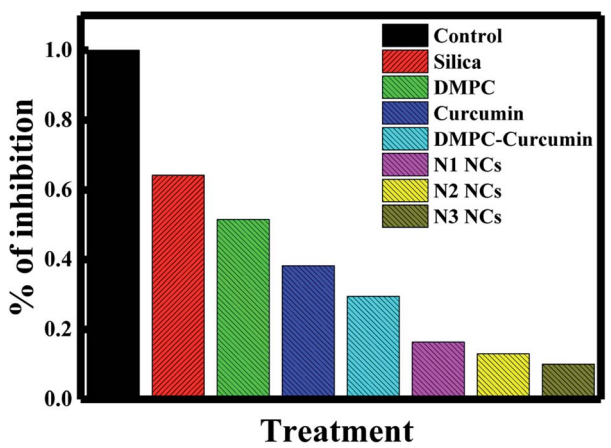

Fig. 7 Effects of silica, DMPC liposomes, curcumin, DMPC–curcumin, N1, N2, and N3 on the inhibition% of MCF-7 cancer cells.

4. Conclusions

To overcome drug leakage and instability, a liposome matrix was modified by applying different layers using a self-assembly procedure; thus, three different kinds of nanocapsule were prepared. The characterization of the nanocapsules *via* SEM, DLS, TGA, XRD, and spectroscopic techniques was successfully carried out. Fluorescence spectra of curcumin showed a blue shift, indicating that curcumin is present in the lipid bilayers. The relative fluorescence efficiency of curcumin was enhanced upon encapsulation in these nanocapsules, boosting its photophysical properties. It was also found that curcumin is strongly entrapped in the lipid bilayer when the surface of the liposome is coated with multiple layers of PDDA. Moreover, the effects of the added PDDA were best understood *via* analyzing the interactions between PDDA and the encapsulated curcumin through XRD, which manifested the variations in the packing structure of curcumin. The study also established that the curative activity of curcumin can be boosted *via* encapsulating it in DMPC liposome-based nanocapsules. It was found that curcumin shows better encapsulation efficiency in the nanocapsule because of electrostatic interactions that inhibit curcumin from being released. The curcumin release from these nanocapsules followed the Higuchi model, and a slow rate of diffusion occurred when the number of layers increased. The cytotoxic effects of the nanocapsules, curcumin, silica, and PDDA were studied with respect to MCF-7 malignant cells. The results demonstrated that the N3 nanocapsules exhibited the highest percentage of cell growth inhibition, with 90% of cells killed within 72 hours. However, lower percentages were revealed for N2 and N1. This is related to the high amount of curcumin accumulated in the core of the N3 capsules, which is attributed to the high encapsulation percentage observed. This study suggests that by applying different layers on the liposome surface, the drug release and anti-cancer activity of curcumin can be enhanced. Further studies involving normal cells and other kinds of cancer cells and animal studies are needed before applying such nanocapsules in drug delivery.

Conflicts of interest

There are no conflicts to declare.

Table 3 Anti-cancer activities of different agents toward the MCF-7 cancer cell line

Cell type	Anti-cancer agent	Concentration	% proliferation	Error margin	References
MCF-7	FA-MTX conjugated Au@SiO_2 NPs	25 μg mL^{-1}	60%	±2.1%	51
	Liposomal curcumin	10 μg mL^{-1}	75%	±0.5%	52
	Nanocapsules	5 μg mL^{-1}	90%	±1.2%	Our work

Acknowledgements

Financial support provided by the American University of Beirut, Lebanon, University of Petra, Jordan, and Kamal A. Shair Central Research Laboratory (KAS CRSL) utilities to proceed this work is extremely appreciated.

References

1 C. Bartolucci, V. Scognamiglio, A. Antonacci and L. F. Fraceto, What makes nanotechnologies applied to agriculture green?, *Nano Today*, 2022, **43**, 1–18.
2 K. Subramani and M. Mehta, *Nanodiagnostics in microbiology and dentistry*, Elsevier Inc., 2nd edn, 2018.
3 R. S. Abdel-Rashid, D. A. Helal, A. A. Alaa-Eldin and R. Abdel-Monem, Polymeric versus lipid nanocapsules for miconazole nitrate enhanced topical delivery: in vitro and ex vivo evaluation, *Drug Delivery*, 2022, **29**(1), 294–304.
4 B. Huang, *et al.*, Preparation, Characterization, and Evaluation of Pyraclostrobin Nanocapsules by In Situ Polymerization, *Nanomaterials*, 2022, **12**(549), 1–10.
5 A. F. Ourique, A. R. Pohlmann, S. S. Guterres and R. C. R. Beck, Tretinoin-loaded nanocapsules: Preparation, physicochemical characterization, and photostability study, *Int. J. Pharm.*, 2008, **352**, 1–4.
6 A. Matsumoto, Polymerization of multiallyl monomers, *Prog. Polym. Sci.*, 2001, **26**(2), 189–257.
7 L. Zhaparova, *Synthesis of nanoparticles and nanocapsules for controlled release of the antitumor drug "Arglabin" and antituberculosis drugs*, 2012.
8 M. C. Fontana, K. Coradini, S. S. Guterres, A. R. Pohlmann and R. C. R. Beck, Nanoencapsulation as a way to control the release and to increase the photostability of clobetasol propionate: Influence of the nanostructured system, *J. Biomed. Nanotechnol.*, 2009, **5**(3), 254–263.
9 S. Khoee and M. Yaghoobian, An investigation into the role of surfactants in controlling particle size of polymeric nanocapsules containing penicillin-G in double emulsion, *Eur. J. Med. Chem.*, 2009, **44**(6), 2392–2399.
10 C. Pinto Reis, R. J. Neufeld, A. J. Ribeiro and F. Veiga, Nanoencapsulation I. Methods for preparation of drug-loaded polymeric nanoparticles, *Nanomedicine*, 2006, **2**(1), 8–21.
11 P. Jagadeesh, S. Dasthagiri and G. Nethravani, Review of nanocapsules, *World J. Pharm. Pharm. Sci.*, 2016, **5**(2), 1365–1380.
12 D. Sharma, A. A. E. Ali and L. R. Trivedi, An Updated Review on: Floating Drug Delivery System (Fdds), *PharmaTutor*, 2011, **6**(2), 50–62.
13 P. Van Hoogevest and A. Wendel, The use of natural and synthetic phospholipids as pharmaceutical excipients, *Eur. J. Lipid Sci. Technol.*, 2014, **116**(9), 1088–1107.
14 A. Akbarzadeh, R. Rezaei-sadabady, S. Davaran, S. W. Joo and N. Zarghami, Liposome: classification, preparation, and applications, *Nanoscale Res. Lett.*, 2013, **8**(102), 1–9.
15 L. Sercombe, T. Veerati, F. Moheimani, S. Y. Wu and S. Hua, Advances and Challenges of Liposome Assisted Drug Delivery, *Front. Pharmacol.*, 2015, **6**(286), 1–13.
16 S. Hua and S. Y. Wu, The use of lipid-based nanocarriers for targeted pain therapies, *Front. Pharmacol.*, 2013, **4**, 1–7.
17 J. Wang, J. Gong and Z. Wei, Strategies for Liposome Drug Delivery Systems to Improve Tumor Treatment Efficacy, *AAPS PharmSciTech*, 2022, **23**(1), 1–14.
18 A. Omri, Z. E. Suntres and P. N. Shek, Enhanced activity of liposomal polymyxin B against Pseudomonas aeruginosa in a rat model of lung infection, *Biochem. Pharmacol.*, 2002, **64**, 1407–1413.
19 C. Quispe, *et al.*, Review Article Therapeutic Applications of Curcumin in Diabetes: A Review and Perspective, *BioMed Res. Int.*, 2022, **15**, 1–14.
20 P. Cornago, R. M. Claramunt, L. Bouissane and I. Alkorta, A study of the tautomerism of b-dicarbonyl compounds with special emphasis on curcuminoids, *Tetrahedron Lett.*, 2008, **64**, 8089–8094.
21 B. B. Aggarwal and K. B. Harikumar, Potential Therapeutic Effects of Curcumin, the Anti Inflammatory Agent, Against Neurodegenerative, cardiovascular, Pulmonary, Metabolic, Autoimmune and Neoplastic Diseases, *Natl. Inst. Health*, 2010, **41**(1), 40–59.
22 D. Lin, *et al.*, Preparation, characterization and antioxidant properties of curcumin encapsulated chitosan/lignosulfonate micelles, *Carbohydr. Polym.*, 2022, **281**, 1–18.
23 B. Saifi, *et al.*, An overview of the therapeutic effects of curcumin in reproductive disorders with a focus on the antiinflammatory and immunomodulatory activities, *Phytother Res.*, 2022, 1–16.
24 A. Rajasekar, T. Devasena, S. Suresh, B. Senthil, R. Sivaramakrishnan and A. Pugazhendhi, Curcumin nanospheres and nanorods: synthesis, characterization and anticancer activity, *Process Biochem.*, 2022, **112**, 248–253.
25 M. Estephan, R. El Kurdi and D. Patra, Curcumin-embedded DBPC liposomes coated with chitosan layer as a fluorescence nanosensor for the selective detection of ribonucleic acid, *Luminescence*, 2022, 1–9.
26 M. Estephan, R. El Kurdi and D. Patra, Interaction of curcumin with diarachidonyl phosphatidyl choline (DAPC) liposomes: chitosan protects DAPC liposomes without changing phase transition temperature but impacting membrane permeability, *Colloids Surf., B*, 2021, **199**, 1–18.
27 L. Bechnak, C. Khalil, R. El Kurdi, R. S. Khnayzer and D. Patra, Curcumin encapsulated colloidal amphiphilic block co-polymeric nanocapsules: colloidal nanocapsules enhance photodynamic and anticancer activities of curcumin, *Photochem. Photobiol. Sci.*, 2020, **19**(8), 1088–1098.
28 S. Shen, T. Wu, Y. Liu and D. Wu, High drug-loading nanomedicines: progress, current status, and prospects, *Int. J. Nanomed.*, 2017, **12**, 4085–4109.
29 R. El Kurdi and D. Patra, Role of OH- in the Fortmation of Hoghly Selective Nanowires at Extreme pH: Multi-fold Enhancement in Rate of Catalytic Reduction Reaction by Gold Nanowires, *Phys. Chem. Chem. Phys.*, 2017, **16**(6), 1–20.
30 L. A. Moreno, Absolute Quantum Yield Measurement of Powder Samples, *J. Visualized Exp.*, 2012, **63**, 1–6.

31 W. Lee, *et al.*, Recent advances in curcumin nanoformulation for cancer therapy, *Expert Opin. Drug Delivery*, 2014, **11**(8), 1183–1201.
32 L. W. Young, *Liposome formulation Having Hydrophilic And Hydrophobic Pharmaceutical Compounds Co-Encapsulated*, 2010.
33 R. El Kurdi and D. Patra, Capping of supramolecular curcubit[7]uril facilitates formation of Au nanorods during pre-reduction by curcumin, *Colloids Surf., A*, 2018, **553**, 97–104.
34 C. Cheng, S. Peng, Z. Li, L. Zou, W. Liu and C. Liu, Improved bioavailability of curcumin in liposomes prepared using a pH-driven, organic solvent-free, easily scalable process, *RSC Adv.*, 2017, **7**(42), 25978–25986.
35 X. Yang, *et al.*, Curcumin-encapsulated polymeric micelles suppress the development of colon cancer in vitro and in vivo, *Sci. Rep.*, 2015, **5**(April), 1–15.
36 R. El Kurdi and D. Patra, Tuning the surface of Au nanoparticles using poly(ethylene glycol)-block-poly(propylene glycol)-block-poly(ethylene glycol): Enzyme free and label free sugar sensing in serum samples using resonance Rayleigh scattering spectroscopy, *Phys. Chem. Chem. Phys.*, 2018, **20**(14), 9616–9629.
37 H. Danafar, *et al.*, Curcumin delivery by modified biosourced carbon-based nanoparticles, *Nanomedicine*, 2022, **17**(2), 95–105.
38 L. Xu, W. Li, S. Sadeghi-Soureh, S. Amirsaadat, R. Pourpirali and S. Alijani, Dual drug release mechanisms through mesoporous silica nanoparticle/electrospun nanofiber for enhanced anticancer efficiency of curcumin, *J. Biomed. Mater. Res., Part A*, 2022, **110**(2), 316–330.
39 S. Roch, A. Rosas-durazo, P. Z. Id and A. Maldonado, Drug Release Properties of Diflunisal from Layer-By-Nanocapsules: Effect of Deposited Layers, *J. Polym.*, 2018, **10**(760), 1–16.
40 T. G. Shutava, P. P. Pattekari, K. A. Arapov, V. P. Torchilin and Y. M. Lvov, Architectural layer-by-layer assembly of drug nanocapsules with PEGylated polyectrolytes, *Natl. Inst. Health*, 2013, **8**(36), 9418–9427.
41 P. Priya, R. M. Raj, V. Vasanthakumar and V. Raj, Curcumin-loaded layer-by-layer folic acid and casein coated carboxymethyl cellulose/casein nanogels for treatment of skin cancer, *Arabian J. Chem.*, 2017, 1–15.
42 S. Honary and F. Zahir, Effect of zeta potential on the properties of nano-drug delivery systems – A review (Part 2), *Trop. J. Pharm. Res.*, 2013, **12**(2), 265–273.
43 N. Raghunand, B. P. Mahoney and R. J. Gillies, Tumor acidity, ion trapping and chemotherapeutics: II. pH-dependent partition coefficients predict importance of ion trapping on pharmacokinetics of weakly basic chemotherapeutic agents, *Biochem. Pharmacol.*, 2003, **66**(7), 1219–1229.
44 B. Vessels, S. Ran, A. Downes and P. E. Thorpe, Increased Exposure of Anionic Phospholipids on the Surface of Tumor, *Cancer Res.*, 2002, **62**(1), 6132–6140.
45 D. Psimadas, P. Georgoulias, V. Valotassiou and G. Loudos, Thermodynamic Modeling of Activity Coefficient and Prediction of Solubility: Part 2. Semipredictive or Semiempirical Models, *J. Pharm. Sci.*, 2012, **101**(7), 2271–2280.
46 S. Cafaggi, *et al.*, Preparation and evaluation of nanoparticles made of chitosan or N-trimethyl chitosan and a cisplatin – alginate complex, *J. Controlled Release*, 2007, **121**, 110–123.
47 E. Joseph and G. Singhvi, *Multifunctional nanocrystals for cancer therapy: A potential nanocarrier*, Elsevier Inc., 2019.
48 T. Higuchi, Mechanism of Sustained-Action Medication, *J. Pharm. Sci.*, 1963, **52**, 1145–1149.
49 G. Pamunuwa, V. Karunaratne and D. N. Karunaratne, Effect of lipid composition on in vitro release and skin deposition of curcumin encapsulated liposomes, *J. Nanomater.*, 2016, 1–9.
50 P. C. Thacker and D. Karunagaran, Curcumin and emodin down-regulate TGF-β signaling pathway in human cervical cancer cells, *PLoS One*, 2015, **10**(3), 1–27.
51 R. Agabeigi, S. H. Rasta, M. Rahmati-Yamchi, R. Salehi and E. Alizadeh, Novel Chemo-Photothermal Therapy in Breast Cancer Using Methotrexate-Loaded Folic Acid Conjugated Au@SiO_2 Nanoparticles, *Nanoscale Res. Lett.*, 2020, **15**(1), 1–14.
52 H. B. Ruttala and Y. T. Ko, Liposomal co-delivery of curcumin and albumin/paclitaxel nanoparticle for enhanced synergistic antitumor efficacy, *Colloids Surf., B*, 2015, **128**, 419–426.